CrossMark

Electroluminescent cooling mechanism in InGaN/GaN light-emitting diodes

Joachim Piprek[1] · Zhan-Ming Li[2]

Abstract GaN-based light-emitting diodes (LEDs) are able to emit photons of higher energy than the injected electrons, resulting in an above-unity electrical efficiency. This phenomenon is generally attributed to heat extraction from the crystal lattice. In good agreement with measurements, we investigate the microscopic mechanism and the magnitude of such electroluminescent cooling by advanced numerical simulation including all relevant heat transfer mechanisms. Peltier cooling near the InGaN light-emitting layer is found to reduce the internal LED temperature rise significantly.

1 Introduction

GaN-based light-emitting diodes (GaN-LEDs) are currently of great interest for applications in lighting, displays, sensing, biotechnology, medical instrumentation and other areas. For more than a decade, intense research and development efforts have been directed towards improving the electrical-to-optical power conversion efficiency PCE of these devices, especially for applications in solid state lighting (Weisbuch et al. 2015). PCE

This article is part of the Topical Collection on Numerical Simulation of Optoelectronic Devices 2016.

Guest edited by Yuh-Renn Wu, Weida Hu, Slawomir Sujecki, Silvano Donati, Matthias Auf der Maur and Mohamed Swillam.

✉ Joachim Piprek
  piprek@nusod.org

[1] NUSOD Institute LLC, Newark, DE 19714-7204, USA

[2] Crosslight Software Inc., 230-3410 Lougheed Hwy, Vancouver, BC V5M 2A4, Canada

   Springer

gives the ratio of light output power to electrical input power and it is also called wall-plug efficiency. However, while much attention is devoted to the GaN-LED efficiency droop with higher current, another phenomenon is hardly discussed in the literature: the surprisingly low turn-on bias V of industry-grade devices. Optimized devices exhibit an electron injection energy qV below the photon emission energy E_{ph} at elevated stage temperature of T = 358 K, up to j = 75 A/cm^2 current density and well beyond the PCE peak at j = 3 A/cm^2 (Hurni et al. 2015). The high photon energy is attributed to the absorption of thermal power by injected electron–hole pairs before they recombine radiatively, resulting in an electrical efficiency ELE = E_{ph}/qV above unity.

This electroluminescent cooling phenomenon was first observed in 1953 on SiC diodes and connected to the Peltier effect (Lehovec et al. 1953). Various experimental and theoretical investigations followed, including numerical drift–diffusion models for heterostructure LEDs that predict the possibility of net cooling with PCE > 1 (Han et al. 2007; Heikkilä et al. 2010; Lee and Yen 2012). Somewhat surprisingly, the actual cooling mechanism is not considered in these models and the net internal heat power is indirectly determined as difference of optical and electrical power. The common assumption of quasi-equilibrium carrier distributions does not reveal how this equilibrium is established. We therefore include the underlying transfer of thermal energy from and to the crystal lattice in our model.

2 Model

Utilizing advanced numerical simulation, we here analyze the electroluminescent cooling mechanism in a realistic GaN-LED and directly identify the local distribution and the magnitude of the Peltier cooling power. We employ the advanced LED device simulation software APSYS which self-consistently computes carrier transport, the wurtzite electron band structure of strained quantum wells (QWs), the photon emission spectrum, as well as heat generation and dissipation. Schrödinger and Poisson equations are solved iteratively in order to account for the quantum well deformation with changing device bias (quantum-confined Stark effect). The carrier transport model includes drift and diffusion of electrons and holes, Fermi statistics, built-in polarization and thermionic emission at hetero-interfaces, as well as Shockley–Read–Hall (SRH) recombination and Auger recombination of carriers.

All relevant heat generation mechanisms are considered self-consistently, i.e., calculated from the local carrier densities and current densities, including Joule heat, heat from non-radiative recombination, as well as the following expression for the Peltier heat power

$$H_{Peltier} = -T(\vec{j}_n \nabla P_n + \vec{j}_p \nabla P_p) \tag{1}$$

with the vectors of the current densities j and the gradients of the thermoelectric power P for electrons and holes, respectively. The thermoelectric power accounts for the excess energy of carriers (in V/K). It is also referred to as Seebeck coefficient and it rises with lower carrier density and with higher temperature (Sztein et al. 2013). Multiplying the Peltier coefficient TP by the charge q gives the average energy transported by electrons or holes with respect to the Fermi energy (Pipe et al. 2002). This excess energy increases when carriers move up a potential barrier, leading to negative Peltier heat (cooling). On the other hand, positive Peltier heat is generated when carriers drop into a quantum well. More details on our models can be found elsewhere (Piprek 2003).

3 Results and discussion

As practical example, our study employs a single-QW blue LED (Galler 2014). Since heat removal is expected to be most effective at elevated temperatures, we here refer to the reported case of T = 400 K stage temperature. Crucial material parameters are extracted by simultaneously fitting measurements of internal quantum efficiency (IQE), photon energy, and bias versus current density (Fig. 1). IQE gives the ratio of photon generation to carrier injection. The simulated carrier leakage from the QW is negligible in this case and the LED efficiency droop at higher current is solely caused by QW Auger recombination. The low-current efficiency is controlled by defect-related SRH recombination. Our IQE fit in Fig. 1 provides the SRH recombination lifetime of 18 ns and the Auger recombination coefficient of $C = 10^{-30}$ cm^6/s which are both close to literature data. The photon generation rate is calculated self-consistently without using the common fit parameter B. The external quantum efficiency EQE = IQE × EXE is further limited by the photon extraction efficiency EXE which depends on the packaging of the LED chip. For simplicity, we here discuss the ideal case of EXE = 1.

The QW interface polarization charge density of 1.3×10^{13} cm^{-2} is obtained by reproducing the blue-shift of the emission wavelength with rising current which is caused by partial screening of the QW polarization field. Accurate calculation of this polarization field is essential for the extraction of the Peltier cooling power.

The fit of the bias-current characteristic in Fig. 1 reveals a contact resistivity of 3×10^{-3} Ωcm^2 for this device which has a negligible influence on our analysis due to the relatively low current density. The simulated bias at low current is slightly higher than measured, possibly due to defect-related tunneling effects (Auf der Maur et al. 2015) which are not considered in our model and which may also lead to the slight overestimation of IQE at low current in Fig. 1. However, in good agreement with the measurement, the simulation results in ELE > 1 up to j = 10 A/cm^2 current density (I = 4 mA). Since ELE is near unity and EXE = 1, PCE = ELE × EXE × IQE is almost identical to the IQE curve in Fig. 1. The PCE peak of 0.57 coincides with ELE = 1.02.

Fig. 1 Comparison between LED measurements (*symbols*) and simulations (*lines*) at 400 K stage temperature. The LED chip size is 200 μm × 200 μm and the maximum current is 40 mA
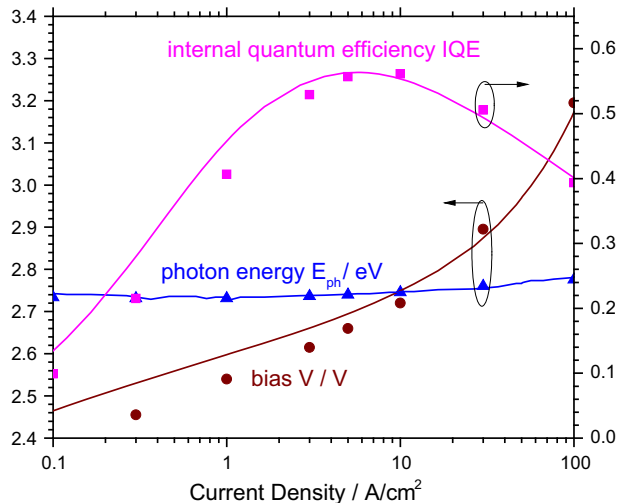
Figure 2 shows the energy band diagram of the single-quantum-well structure at low current including the quantum well energy levels and wave functions. Built-in polarization causes a strong deformation of the QW and contributes to the triangular potential barrier which electrons and holes need to climb up before entering the active layer. The carriers captured in the lowest QW level have a higher energy difference ($\Delta E_1 = 2.745$ eV) than the quasi-Fermi levels ($\Delta E_F = 2.452$ eV) at $j = 0.1$ A/cm^2. This results in the emission of blue photons while the applied bias is still lower than E_{ph}/q, as shown in Fig. 1. Photon energy and $qV = 2.746$ eV are identical near $j = 10$ A/cm^2 but $\Delta E_F = 2.689$ eV is still lower. But at $j = 100$ A/cm^2 the QW quasi-Fermi level splitting $\Delta E_F = 2.811$ eV finally exceeds the photon energy $E_{ph} = 2.783$ eV.

Carriers climbing up the energy hill towards the QW do so by acquiring thermal energy from the crystal lattice (Peltier cooling). Subsequently, Peltier heating happens when carriers fall into the QW and transfer part of the thermal energy back to the lattice. Figure 3

Fig. 2 Energy band diagram near the InGaN/GaN quantum well (QW; *EBL*—electron blocking layer; *dashed* quasi Fermi levels, *red* quantum levels and wave functions, current density $j = 0.1$ A/cm^2). (Color figure online)
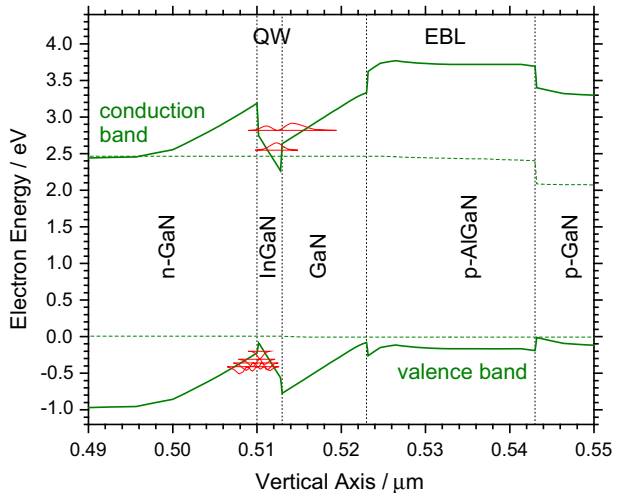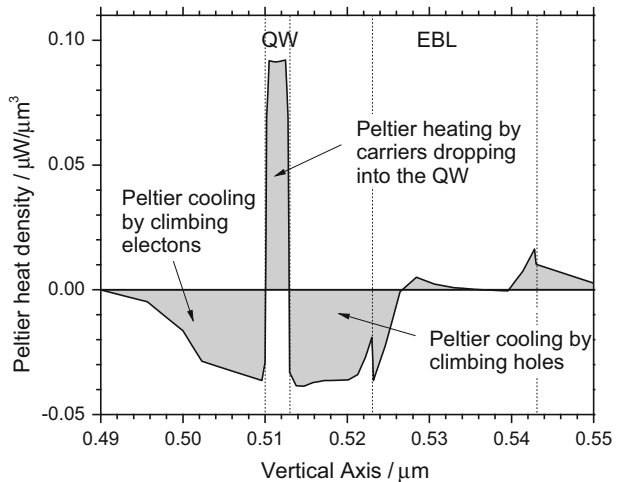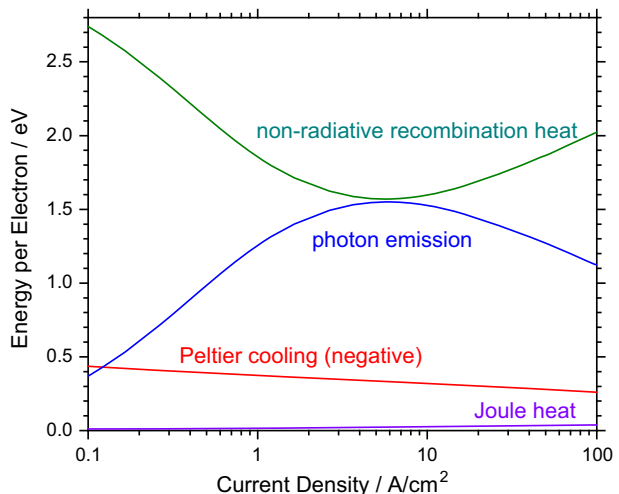

Fig. 3 Vertical Peltier heat profile near the quantum well (QW, *EBL*—electron blocking layer, $j = 0.1$ A/cm^2)

shows the simulated Peltier heat profile near the QW. Most of the heat extraction occurs in the QW barriers but some also in the EBL. Figure 4 plots the net Peltier cooling energy per injected electron in comparison to other processes. The cooling per carrier slightly declines with higher current since the QW potential barrier is reduced with higher bias. But the net Peltier heat is negative even at higher current because the average energy difference between electrons and holes inside the QW remains larger than the quantum level difference ΔE_1 which controls the photon energy. In other words, carriers entering the QW lose less average excess energy than they gained by climbing up to it. This contradicts a recently published analytical model which simply extracts the Peltier heat from the difference of optical and electrical power (Xue et al. 2015). However, the Peltier cooling is substantially smaller than the heating by non-radiative recombination inside the QW, which is dominated by SRH recombination at low currents and by Auger recombination at high currents (for simplicity, we here assume that hot Auger carriers transfer their energy to the lattice within the QW). In between, as photon generation exhibits the highest probability IQE, the emitted photon energy per injected electron peaks. Joule heat is mainly controlled by the free hole density (10^{18} cm^{-3}) and the hole mobility (10 cm^2/Vs) and it remains negligible at our low current density. At our peak quantum efficiency IQE = EQE = 0.56, the Peltier cooling reduces the total heat power by about 20 %. Electroluminescent refrigeration (PCE > 1) would require a peak EQE > ELE^{-1} = 0.98 in this case.

The internal temperature rise depends on the total heat power and the total thermal resistance R_{th} of the packaged LED. We here assume R_{th} = 50 K/W and calculate the QW temperature rise with and without Peltier effect (Fig. 5). For this comparison, we remove the Peltier heat (1) from the heat flux equation, but the carriers still gain the same excess energy before dropping into the QW. At j = 100 A/cm^2 and EXE = 1, the Peltier cooling reduces the internal temperature rise by about 20 %, from 4.8 to 3.8 K. For such low temperature rise, the cooling effect on other LED performance parameters is negligible and the IQE characteristics are identical in both cases (solid line in inset of Fig. 5). However, our reference LED is relatively small (200 μm × 200 μm). A large-area LED (1 mm × 1 mm) would generate 25 times the heat power at the same current density, leading to 25 times the internal temperature rise with and without Peltier cooling.

Fig. 4 Energy distribution per injected electron versus current density

The Peltier cooling should be higher within LEDs employing multiple QWs since carriers climb up the energy hill towards the QW multiple times. We here add two more QWs to our reference device and show the results in Figs. 5 and 6 (dashed lines). The Peltier cooling power clearly rises. However, while most carriers accumulate in the p-side QW, the carrier density in each QW is smaller than in the original LED at any given current, the overall Auger recombination is reduced, the efficiency at higher current is improved (dashed line in inset of Fig. 5), and the output power rises. Thus, the reduction in total self-heating (dashed line in Fig. 5) is caused both by the increased Peltier cooling and by the reduced Auger recombination.

In comparison, a single 9 nm thick QW produces a slightly reduced Peltier cooling power (dash-dot line in Fig. 6) but the QW carrier density is about three times lower than in the reference LED so that the influence of Auger recombination declines even further. The heat power reduction is almost the same as with 3 QWs but it is now caused by the

Fig. 5 Quantum well temperature versus current density as calculated with (*solid red*) and without Peltier cooling effect (*solid blue*) for a thermal resistance of 50 K/W (*dashed* 3 QWs, *dash-dot* 9 nm thick QW, *inset* corresponding internal quantum efficiency). (Color figure online)
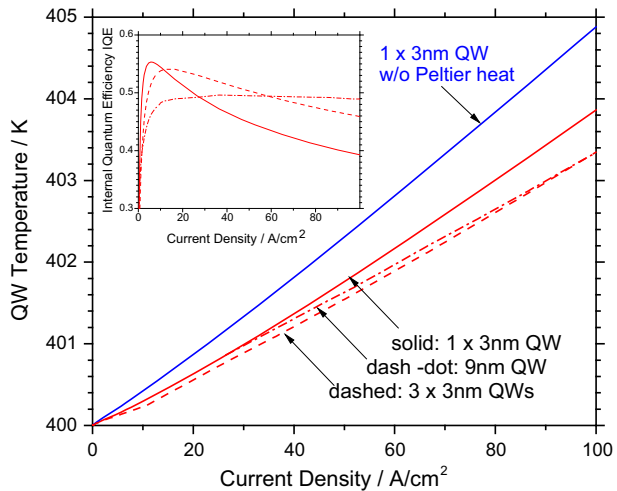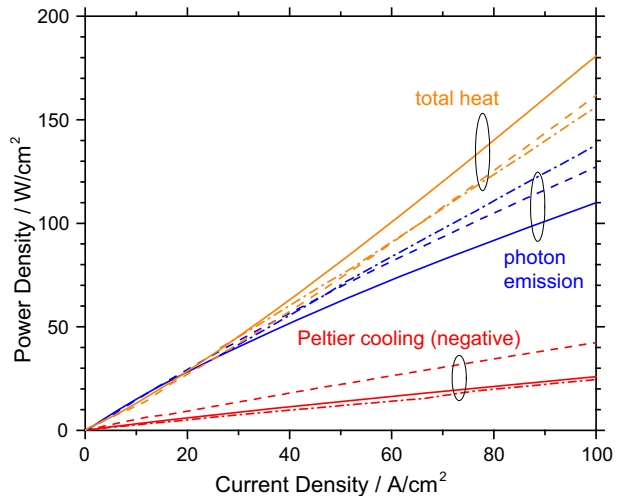

Fig. 6 Peltier power, total heat power, and light output power versus current density for different active regions (*solid* original 3 nm QW, *dash-dot* 9 nm QW, *dashed* 3 × 3 nm QWs)

reduced Auger recombination and not by enhanced Peltier cooling. The IQE droop is almost eliminated (dash-dot line in inset of Fig. 5). Thus, a promising strategy for reduced heat production at high current is the same as for efficiency droop suppression, namely the reduction of the QW carrier density, which reduces carrier losses.

4 Summary

We have identified the mechanism and the magnitude of electroluminescent cooling in a realistic single-quantum well InGaN/GaN blue LED using advanced device simulation. The built-in polarization field clearly enhances the Peltier cooling effect which reduces the internal temperature rise by up to 20 %, depending on the photon extraction efficiency.

References

Auf der Maur, M., Galler, B., Pietzonka, I., Strassburg, M., Lugauer, H., Di Carlo, A.: Trap-assisted tunneling in InGaN/GaN single-quantum-well light-emitting diodes. Appl. Phys. Lett. **105**, 133504 (2015)

Galler, B.T.: Ph.D. Thesis, Albert Ludwigs University, Freiburg, Germany, 2014 (in German)

Han, P., Jin, K., Zhou, Y.-L., Lu, H.-B., Yang, G.-Z.: Numerical designing of semiconductor structure for optothermionic refrigeration. J. Appl. Phys. **101**, 014506 (2007)

Heikkilä, O., Oksanen, J., Tulkki, J.: The challenge of unity wall plug efficiency: the effects of internal heating on the efficiency of light emitting diodes. J. Appl. Phys. **107**, 033105 (2010)

Hurni, C.A., David, A., Cich, M.J., Aldaz, R.I., Ellis, B., Huang, K., Tyagi, A., DeLille, R.A., Craven, M.D., Steranka, F.M., Krames, M.R.: Bulk GaN flip-chip violet light-emitting diodes with optimized efficiency for high-power operation. Appl. Phys. Lett. **106**, 031101 (2015)

Lee, K.C., Yen, S.T.: Photon recycling effect on electroluminescent refrigeration. J. Appl. Phys. **111**, 014511 (2012)

Lehovec, K., Accardo, C.A., Jamgochian, E.: Light emission produced by current injected into a green silicon-carbide crystal. Phys. Rev. **89**, 20–25 (1953)

Pipe, K.P., Ram, R.J., Shakouri, A.: Bias-dependent Peltier coefficient and internal cooling in bipolar devices. Phys. Rev. **66**, 125316 (2002)

Piprek, J.: Semiconductor Optoelectronic Devices—Introduction to Physics and Simulation. Academic Press, San Diego (2003)

Sztein, A., Haberstroh, J., Bowers, J.E., DenBaars, S.P., Nakamura, S.: Calculated thermoelectric properties of InxGal − xN, InxAl1 − xN, and AlxGa1 − xN. J. Appl. Phys. **113**, 183707 (2013)

Weisbuch, C., Piccardo, M., Martinelli, L., Iveland, J., Peretti, J., Speck, J.S.: The efficiency challenge of nitride light-emitting diodes for lighting. Phys. Status Solidi A **212**, 899–913 (2015)

Xue, J., Zhao, Y., Oh, S.-H., Herrington, W.F., Speck, J.S., DenBaars, S.P., Nakamura, S., Ram, R.J.: Thermally enhanced blue light-emitting diode. Appl. Phys. Lett. **107**, 121109 (2015)